TR # 251

SUPERCOMPUTER SIMULATION OF SESSILE AND PENDENT DROPS *

by

Donald Greenspan

Abstract

A quasimolecular approach is developed for the modelling of sessile and pendent drops. Fundamental mechanisms of drop formation are formulated in terms of gravity and classical intermolecular type forces. CRAY X-MP/24 computer examples illustrate standing and falling drops, free surface motions, and convergence to equilibrium. The role of temperature in drop configuration modelling is shown to be significant.

---

* Computations were performed at the University of Texas Center for High Performance Computing

1. Introduction. The study of fluid drops has long been of interest to mathematicians, scientists and engineers (see, e.g., refs. 1-5, 9, 10, 13-15, and the numerous references contained therein). Though it seems apparent that surface tension and air resistance are fundamental to the equilibrium shape of a freely falling drop, the developmental mechanisms of drops which stand on or fall from a horizontal, solid surface are less clear. Our primary purpose, then, is to develop such a set of mechanisms which are founded on classical molecular mechanics. When the drop is on top of the surface it is called a sessile drop, when below, a pendent drop. Classically, such drops have been modelled, primarily, only in the equilibrium state and from a continuum point of view, with severe symmetry and homogeneity assumptions imposed (4,5). Our approach will be distinctly different in that it will be discrete and dynamical, will allow for inhomogeneities, and will allow for the evolution of free surfaces.

2. Mathematical, Physical and Modelling Preliminaries. The gross physical motion of a fluid is, primarily, the result of forces due to gravity and due to molecular interaction. Gravity acts uniformly on all molecules in a fluid. Molecular interaction forces are local, or short range, forces which have components of both attraction and repulsion. Classically, these forces have magnitude F given by

$$F = -\frac{G}{r^p} + \frac{H}{r^q} \quad , \quad G>0,\ H>0,\ q>p>7 \quad , \tag{2.1}$$

where r is the radius from P to a neighboring molecule. Because of the singularity in (2.1) at r = 0, the motion of an individual molecule can be relatively volatile locally, even though the gross motion of the fluid is physically stable.

To simulate fluid motion qualitatively, we proceed as follows. First, we group the large number of fluid molecules which are physically present into a relatively small number of larger units called quasimolecules, or particles. This process of lumping molecules into particles is the same as that utilized by both Boussinesq and Prandtl (11,12). Next, we define the motion of each particle, denoted by P_i, of the resulting system of, say, N particles, by the coupled system of nonlinear, ordinary differential equations

$$\vec{F}_i = m_i \ddot{\vec{r}}_i \quad , \quad i=1,2,\ldots,N, \tag{2.2}$$

in which m_i is the mass of P_i. In (2.2),

$$\vec{F}_i = \vec{F}_{1,i} + \vec{F}_{2,i} \quad ,$$

where $\vec{F}_{1,i}$ is the force due to gravity and $\vec{F}_{2,i}$ is the force on P_i due to molecular interaction with its immediate neighbors. The force $\vec{F}_{1,i}$ applies uniformly to all particles P_i, i=1,2,...,N. The force $\vec{F}_{2,i}$ is determined in accordance with (2.1), but with p and q diminished appropriately in order to maintain the physical stability of the gross motion of the system.

Next, the resulting differential system (2.2) is solved numerically from given initial data as follows (6). Consider N particles P_i, i=1,2,...,N. For $\Delta t > 0$, let $t_k = k\Delta t$, k=0,1,2,... . For each i, let m_i denote the mass of P_i and let P_i at t_k be located at $\vec{r}_{i,k} = (x_{i,k}, y_{i,k})$, have velocity $\vec{v}_{i,k} = (v_{i,k,x}, v_{i,k,y})$ and have acceleration $\vec{a}_{i,k} = (a_{i,k,x}, a_{i,k,y})$. Let position, velocity and acceleration be related by the formulas

$$\vec{v}_{i,\frac{1}{2}} = \vec{v}_{i,0} + \tfrac{1}{2}(\Delta t)\vec{a}_{i,0} \tag{2.3}$$

$$\vec{v}_{i,k+\frac{1}{2}} = \vec{v}_{i,k-\frac{1}{2}} + (\Delta t)\vec{a}_{i,k} \quad , \quad k=1,2,\ldots \tag{2.4}$$

$$\vec{r}_{i,k+1} = \vec{r}_{i,k} + (\Delta t)\vec{v}_{i,k+\frac{1}{2}} \quad , \quad k=0,1,2,\ldots \quad . \tag{2.5}$$

At t_k, let the force acting on P_i be $\vec{F}_{i,k}=(F_{i,k,x},F_{i,k,y})$. We relate force and acceleration by the dynamical equation

(2.6) $\vec{F}_{i,k}=m_i\vec{a}_{i,k}$.

The motion of each P_i will be determined explicitly and recursively by (2.3)-(2.6) from given initial data once the force $\vec{F}_{i,k}$ is prescribed, and this is done as follows. First, fix a positive parameter D, called the local distance parameter. Any particle P_j, different from P_i, which lies within a circle of radius D and center P_i is called a neighbor of P_i. If P_j is a neighbor of P_i, let $\vec{r}_{ij,k}$ be the vector from P_i to P_j at time t_k, so that $r_{ij,k} = \| \vec{r}_{i,k}-\vec{r}_{j,k} \|$ is the distance between the two particles. Then the local force $\vec{F}^*_{ij,k}$ on P_i due to P_j at time t_k is defined by

(2.7) $$\vec{F}^*_{ij,k} = \left[-\frac{G}{(r_{ij,k})^p} + \frac{H}{(r_{ij,k})^q} \right] \frac{\vec{r}_{ji,k}}{r_{ij,k}} \quad .$$

The total force $\vec{F}^*_{i,k}$ on P_i at t_k is defined by

(2.8) $$\vec{F}^*_{i,k} = \sum_{\substack{j=1 \\ j\neq i}} \vec{F}^*_{ij,k} \quad ,$$

where the summation is taken over all neighbors of P_i. Finally, the total force $\vec{F}_{i,k}$ on P_i at t_k is defined by

(2.9) $F_{i,k,x}=F^*_{i,k,x}$, $F_{i,k,y}=F^*_{i,k,y}-m_i g$,

where g is the constant of acceleration due to gravity.

For the convenience of the reader, CRAY FORTRAN programs and data sets to be discussed are available in Greenspan (7) .

3. Examples of Sessile Drop Formation. In order to study sessile drop development, let us begin with a particle fluid in a basin. As described in Greenspan (7,8), we will utilize the 2500 particle fluid shown in Figure 1, which was generated using the scaled parameters p=3, q=5, G=25, H=10, g=9.8, $m_i \equiv 1$, Δt=0.001, D=1.4. (All positions and velocities are available in Greenspan (7).) In order to allow wall adhesion, however, we will replace the straight line boundaries shown in Figure 1 by a set of 405 boundary particles as follows. Let the points A, B, C, D in Figure 2 have respective coordinates (-0.25,25.0), (-0.25,-0.25), (50.25,-0.25), (50.25,25.0). Set a particle at each of A, B, C, D, and set additional particles between A and B, between B and C, and between C and D, so that the spacing between any two consecutive particles is 0.25 units. The resulting set of 405 particles is called the set of solid, or wall, particles.

Of the total 2905 particles, only the 2500 fluid ones will be allowed to move. However, any two particles of the set of 2905 will be allowed to interact locally whenever their distance of separation is less than parameter value D. It is by this means that we will implement wall adhesion. Indeed, when fluid particle P_i has solid particle P_j as a neighbor, the force $\vec{F}_{ij}$ on P_i due to P_j is taken to have magnitude

$$F_{ij} = -\frac{G^*}{(r_{ij,k})^{p^*}} + \frac{H^*}{(r_{ij,k})^{q^*}} .$$

Thus, local interaction of two fluid particles is characterized by the parameters p, q, G, H, while local interaction of a fluid and a solid particle is characterized by p*, q*, G*, and H*.

Throughout the remainder of this paper, we set p=p*=3, q=q*=5, and assume that every particle is of unit mass. Throughout the remainder of this section we set D=1.4.

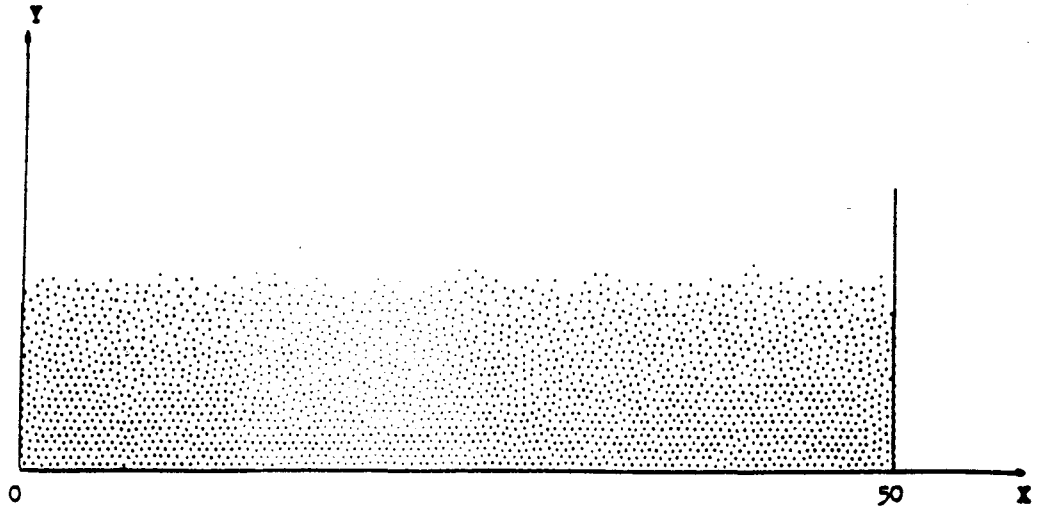

Figure 1

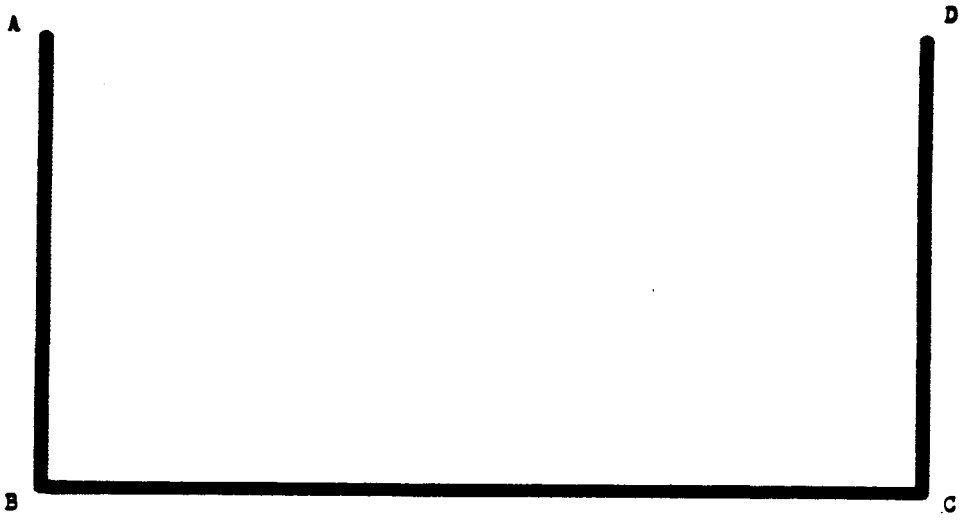

Figure 2

Example 1. In order to induce contraction into the basin fluid, we now set G=100, H=20, G*=H*=0.5, g=9.98, Δt=0.0002. The resulting particle motions were computed for 25000 time steps, that is, to T=5. Figures 3-5 show the contraction stages at T=1.4, 2.8, and 5.0, respectively. Figure 3 shows large particle concentrations at the left and right ends whose motions are toward the center. Each figure reveals particle emissions during the contraction. Figure 5 reveals a relatively amorphous, almost convex particle concentration. The kinetic energy of each system in Figures 3-5 is, approximately, $(325)10^3$ units. We proceed then to "cool" the system shown in Figure 5 and form a sessile drop as follows. The parameters g and Δt are reset to g=9.8, Δt=0.0005 and the simulation is continued for an additional 6000 steps, that is, to T=8. However, at T=5.0, 5.5, 6.0, 6.5, 7.0, and 7.5, the velocity of each particle is reduced by multiplying each component by 0.2, that is, to one fifth of their magnitudes. The resultant drop formation is shown in Figures 6-11, at the respective times T=5.5, 6.0, 6.5, 7.0, 7.5, 8.0. The approximate kinetic energies of the systems shown in Figures 6-11 are, respectively, $(200)10^3$, $(147)10^3$, $(103)10^3$, $(64)10^3$, $(36)10^3$, $(23)10^3$, which is a dramatic decrease from the kinetic energy of the system in Figure 5. All the figures reveal that allowable particle configurations are related directly to the system kinetic energy, or, equivalently, to the fluid temperature. It should be noted also that the fluid particles exhibit vibrational motions at all times, in complete consistency with the molecular theory of matter.

Example 2. To demonstrate the ease with which nonhomogeneities can be treated, let us consider the system of Figure 11 at T=8 and now reset

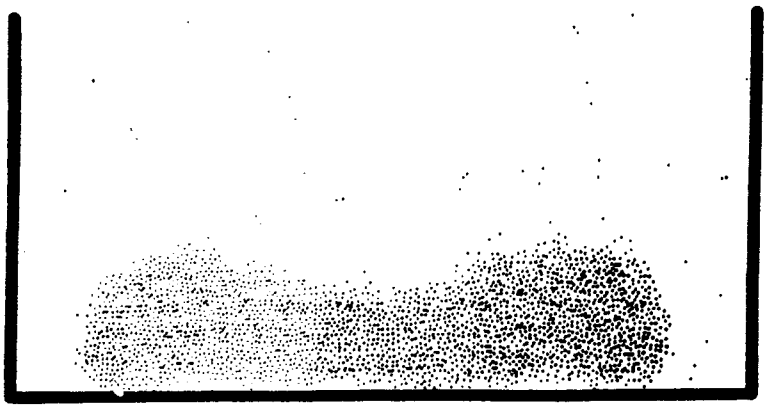

Figure 3

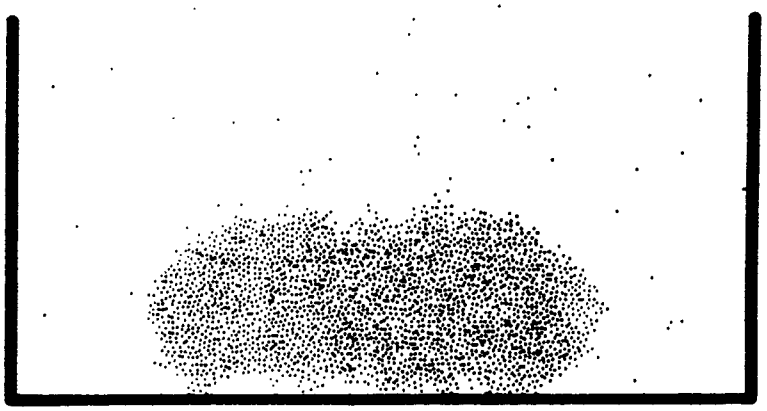

Figure 4

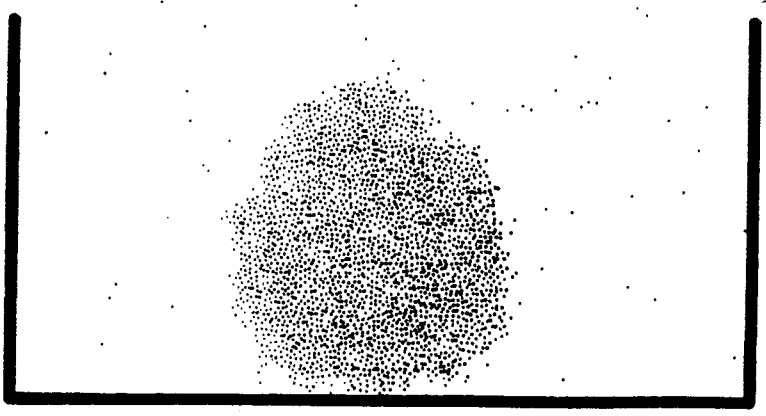

Figure 5

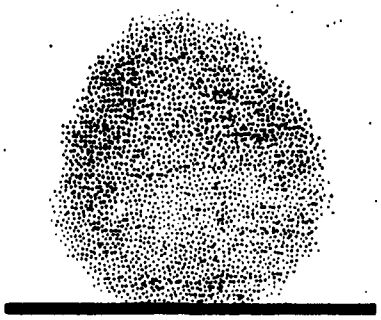

Figure 6

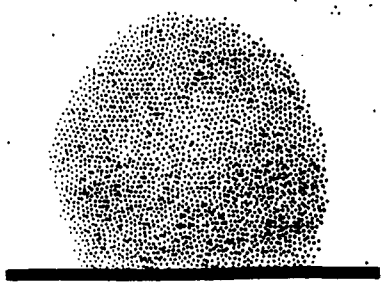

Figure 7

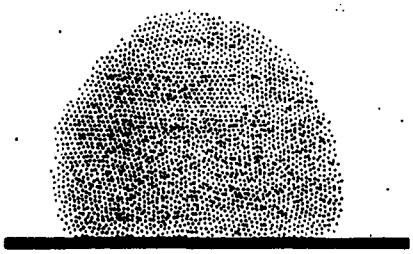

Figure 8

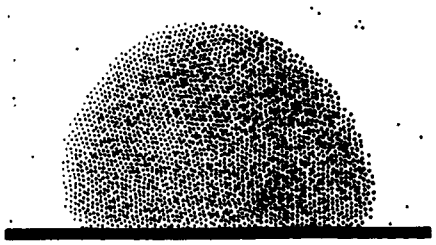

Figure 9

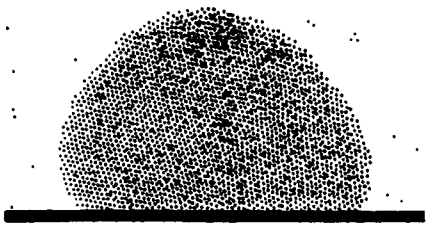

Figure 10

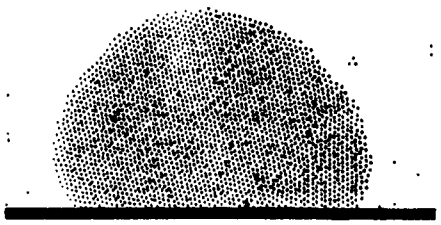

Figure 11

the following parameters. Of the 203 particles in the base BC of Figure 2, let G*=H*=1.0 for the left 101 particles and G*=20, H*=1 for the right 102 particles. Then, continuing the simulation with $\Delta t=0.0005$ for 4000 time steps with the velocity reduction factor 0.2 replaced by 0.95 every 1000 steps results in the system reorganizations shown in Figures 12 and 13 at T=8.5 and T=10.0, respectively. The results

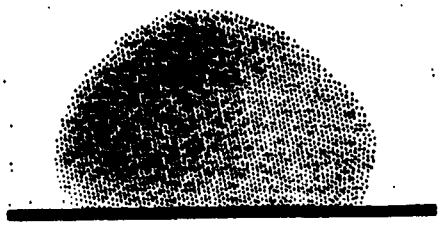

Figure 12

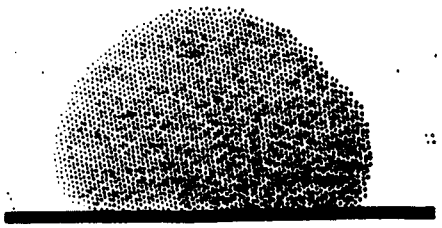

Figure 13

at T=9.0 and 9.5 were essentially identical to that shown in Figure 13, which reveals a skewing of the drop and an increase in vertical contact direction on the right side, in addition to a decrease in vertical contact direction on the left side.

4. Examples of Pendent Drop Formation. To simulate pendent drops, let us again begin with the fluid-solid configuration of Figures 1 and 2. Next, let us invert the entire system of 2905 particles. Then, since the side walls are no longer necessary to contain the fluid, let us eliminate the solid particles of AB and CD, retaining only the 203 solid particles in BC. Our initial configuration, then, is shown in Figure 14 and consists of 2703 particles.

Example 1. To induce contraction, set G=200, H=80, G*=250, H*=100, g=9.8, D=5.0, Δt=0.0002. Then, Figures 15-23 show the resultant drop formation and fall from the surface at the respective times T=0.6, 1.0, 1.4, 1.8, 2.6, 3.6, 4.0, 4.2, and 4.4. At T=2.6, shown in Figure , it becomes clear that an effective downward force dominates. As the neck thins in Figures 20 and 21 the main body of the drop elongates. However, when the main body separates, both it and the neck contract, as shown in Figures 22 and 23 the neck back to the surface and the main body back from its elongated shape.

Fig. 14

Fig. 15

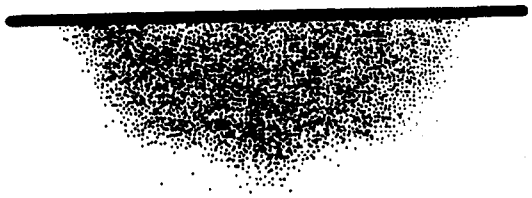

Fig. 16

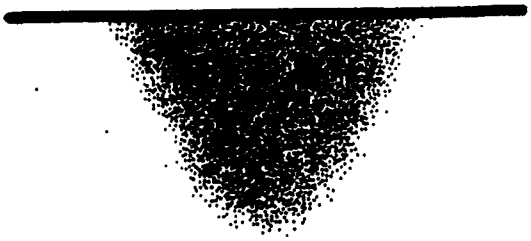

Fig. 17

Fig. 18

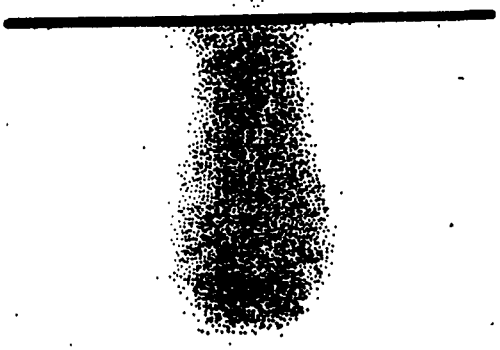

Fig. 19

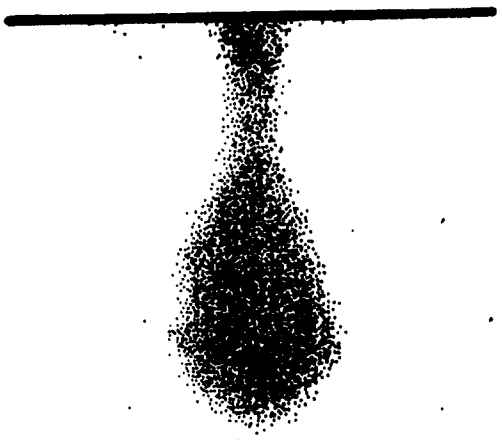

Fig. 20

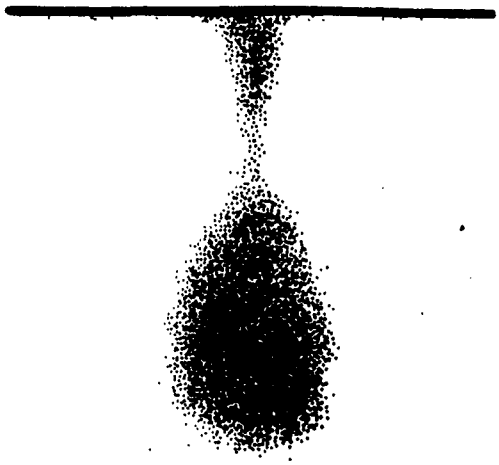

Fig. 21

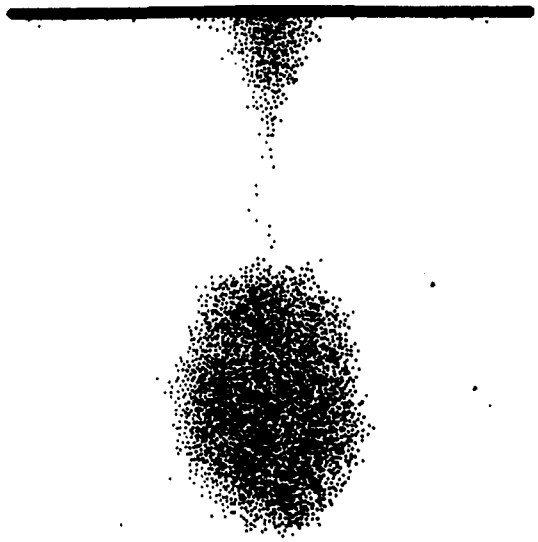

Fig. 22

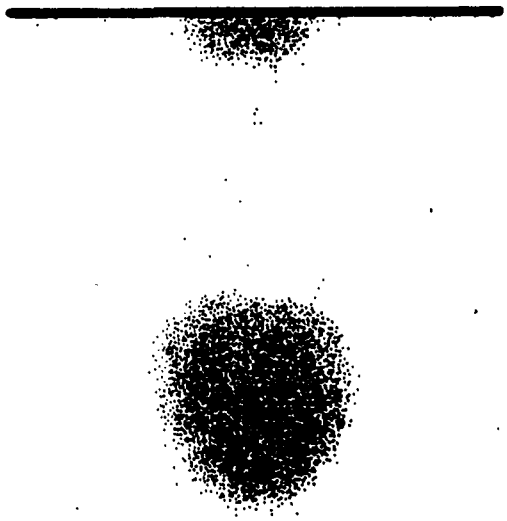

Fig. 23

Fig. 24

Fig. 27

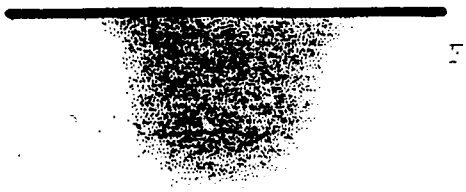

Fig. 25

Fig. 28

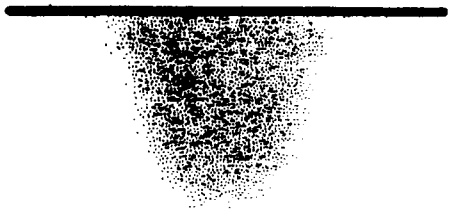

Fig. 26

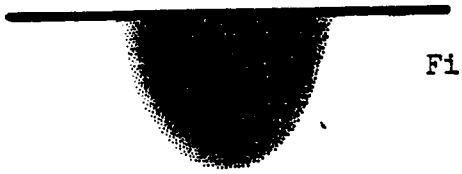

Fig. 29

Example 2. In order to simulate a pendent drop which adheres to the surface, we merely change the gravity constant in Example 1, above, to g=0.98 and rerun the simulation. (Of course, the same effect can be achieved by keeping g=9.8 but resetting the fluid particle masses to 0.1.) Then, Figures 24-27 show the resulting pendent drop formation on the surface at the same times as those corresponding to Figures 16,18,19,20. The contraction this time yields a drop formation which is oscillating toward a steady state. In order to converge to an equilibrium position quickly, we then continued the simulation but with the introduction of the cooling technique described in Example 1 of Section 3. Figures 28 and 29 show the results after 1000 and 4000 time steps, respectively. The kinetic energy of the system in Figure 27 was $(815)10^{-3}$, while that in

Figure 29 is only $(63)10^3$. The relative equilibrium is observed readily by comparing Figures 28 and 29 both of which are in agreement with experimental steady state results (5).

5. Remarks. A large number of related computations were carried out and the results can be summarized as follows. Relatively arbitrary parameter choices usually resulted in an explosion of the system. Nonphysical results usually followed for choices of G, H, G*, H* greater than 1000 or for $\Delta t > 0.001$. Small perturbations of the parameter sets described in Sections 3 and 4 invariably yielded small perturbations in the results described.

It is also interesting to note that the use of higher order numerical techniques for the solution of ordinary differential systems offers little advantage. The reason is that the physics of intermolecular forces does not allow one to choose large values of Δt, since large Δt would allow particles to come too close in a single time step, thus yielding excessively large forces of repulsion.

As to other concepts of interest, like contact angle size and direction, our approach can be implemented by choosing fluid particles at the outer sections of the fluid-solid contacts and employing a least square linear fit. This is practical, however, only when the fluid particle oscillations are relatively small, that is, near steady state.

Finally, we wish to remark about the versatility of our methodology. Any molecular type approach allows for system self-reorganization an attribute not usually available in continuum models. Thus, our approach lends itself readily to questions of how the system responds to various parameter changes.

REFERENCES

1. W. N. Bond, "Bubbles and drops and Stokes' law", Phil. Mag., 4 (1927) p. 889.

2. J. Boussinesq, "Contribution to the theory of capillary action with an extension of viscous forces to the surface layers of liquids and an application notably to the slow uniform motion of a spherical fluid drop", Comp. Rend., 156 (1913) p. 1124.

3. H. L. Dryden, F. D. Murnaghan and H. Bateman, HYDRODYNAMICS , Dover, N.Y., 1956.

4. R. Finn, "Global size and shape estimates for symmetric sessile drops", J. Reine Angew. Math., 335 (1982) p. 9.

5. R. Finn, EQUILIBRIUM CAPILLARY SURFACES, Springer-Verlag, N.Y., 1986.

6. D. Greenspan, ARITHMETIC APPLIED MATHEMATICS, Pergamon, Oxford, 1981.

7. D. Greenspan, "Computer files for drop formation", TR 249 , Math. Dept., Univ. Texas at Arlington, 1988.

8. D. Greenspan, "Computer studies of particle modeling of fluid phenomena", Math. Modelling, 6 (1985) p. 273.

9. K. Hida and T. Nakanishi, "The shape of a bubble or a drop attached to a flat plate", J. Phys. Soc. Japan, 28 (1970) p. 1336.

10. L. Prandtl, "The air resistance of spheres", Nachr. Ges. Wiss., Gottingen (1914) p. 177.

11. L. Prandtl, "On the development of turbulence", ZAMM, 5 (1925) p. 136.

12. H. Schlichting, BOUNDARY LAYER THEORY, McGraw-Hill, N.Y., 1960.

13. G. C. Simpson, "Water in the atmosphere", Nature, 111 (1923) p. 520.

14. W. Thomson (Lord Kelvin), "Capillary attraction", Nature, 34 (1886) p. 270.

15. H. C. Wente, "The symmetry of sessile and pendent drops", Pacific J. Math., 88 (1980) p. 387.